

Spin diffusion in liquid ^3He confined in nafen

V. V. Dmitriev¹⁾, L. A. Melnikovsky, A. A. Senin, A. A. Soldatov, A. N. Yudin

P. L. Kapitza Institute for Physical Problems RAS, 2 Kosygina str., 119334 Moscow, Russia

Submitted 15 May 2015

We report results of spin diffusion measurements in normal phase of liquid ^3He confined in nafen. Nafen is a new type of aerogel and it consists of Al_2O_3 strands which are nearly parallel to one another at macroscopic distances. We examine two samples of nafen with different porosities using spin echo techniques. Spin diffusion of ^3He along and across the strands was measured. The aerogel alignment is clearly evident from observed spin diffusion anisotropy. A theory describing this effect is developed and compared with the experiment.

1. INTRODUCTION

Superfluid ^3He in high porosity aerogel is a model system to investigate the influence of impurities on unconventional superfluidity. Silica aerogels which consist of a nearly chaotic array of SiO_2 strands are used in most of such experiments. An important parameter for theoretical models of superfluid ^3He in aerogel is the mean free path (λ) of Fermi-liquid quasiparticles which can be determined from measurements of spin diffusion coefficient (D). At high temperatures ($T \gtrsim 20$ mK) the density of quasiparticles is large, so λ and D follow the bulk Fermi-liquid behavior, i.e. $\lambda \propto T^{-2}$ and $D \propto T^{-2}$. At low enough temperatures ($T < 10$ mK) aerogel strands limit the mean free path and the spin diffusion coefficient, so that at $T \sim 1$ mK the density of quasiparticles is so small that values of λ and D are fully determined by the array of aerogel strands and do not depend on T . Such behavior was observed in the first measurements of spin diffusion in ^3He confined in nearly isotropic 95% and 98% open silica aerogels [1, 2]. In some recent experiments with superfluid ^3He in aerogel a new type of aerogel was used [3, 4, 5]. The remarkable feature of this aerogel, called “nematically ordered” (N-aerogel), is that its strands are oriented along the same direction. There are two types of N-aerogel: “Obninsk aerogel” produced by Leypunsky Institute (Obninsk, Russia) [6] which consists of AlOOH strands and nafen [7] which consists of Al_2O_3 strands. In the limit of $T = 0$ the strong global anisotropy of N-aerogel should result in anisotropy of ^3He spin diffusion. For example, in “Obninsk aerogel” with overall density ~ 30 mg/cm³ the spin diffusion along the strands is about twice as fast as that in perpendicular direction [8].

Here we present results of the spin diffusion measurements in ^3He confined in nafen, which is much denser than “Obninsk aerogel” and compare the obtained results with the theory we developed.

2. THEORY

An approximate description for the weak field spin diffusion in bulk ^3He was first given by D. Hone [9]

$$j_{\mathbf{M}}^l = -\frac{v_F \lambda}{3} (1 + F_0^a) \frac{\partial \mathbf{M}}{\partial x^l}, \quad (1)$$

where \mathbf{M} is the magnetization, $\mathbf{j}_{\mathbf{M}}$ is respective current, v_F is the Fermi velocity, F_0^a is the Landau Fermi-liquid parameter, and λ is a quasiparticle mean free path. Diffusion in anisotropic aerogel is described by a generalized equation

$$j_{\mathbf{M}}^l = -D^{lm} \frac{\partial \mathbf{M}}{\partial x^m}, \quad (2)$$

where D^{lm} is the spin diffusion tensor. It is important to note, that no mean free path can characterize diffusion in anisotropic medium. Diffusive flux (2) in such system depends on the gradient direction and they are not necessarily parallel to each other. On the other side, a mean free path is a scalar, it is by its nature averaged over quasiparticle distribution which is isotropic even in anisotropic aerogel.

Suppose that the stationary kinetic equation

$$\frac{\partial n}{\partial x^m} \frac{\partial \epsilon}{\partial p^m} - \frac{\partial n}{\partial p^m} \frac{\partial \epsilon}{\partial x^m} = I[n], \quad (3)$$

holds separately for each individual spin component. In the left hand side of the kinetic equation (3) a local equilibrium function should be substituted. This gives [9]

$$\frac{\partial n}{\partial x^m} \frac{\partial \epsilon}{\partial p^m} - \frac{\partial n}{\partial p^m} \frac{\partial \epsilon}{\partial x^m} = -\psi^m \frac{\partial n_0}{\partial \epsilon} \frac{\partial \epsilon}{\partial p^m},$$

where

$$\psi^m = (1 + F_0^a) \frac{2\pi^2 \hbar^3}{p_F m^*} \frac{\partial M}{\partial x^m}.$$

The magnetization here and below is taken in magneton units $\gamma \hbar = 1$.

Calculation of D^{lm} is greatly simplified at low temperature so that the collisions between Fermi quasiparticles can be neglected. This means that the scattering

¹⁾e-mail: dmitriev@kapitza.ras.ru

of quasiparticles on the aerogel alone is responsible for the collision integral

$$I[n] = \int d\mathbf{p}' (w(\mathbf{p}, \mathbf{p}')n'(1-n) - w(\mathbf{p}', \mathbf{p})n(1-n')),$$

where $n = n(\mathbf{p})$, $n' = n(\mathbf{p}')$, and $w(\mathbf{p}, \mathbf{p}') = w(\mathbf{p}', \mathbf{p})$ is the scattering $\mathbf{p}' \rightarrow \mathbf{p}$ probability. Since the scattering by aerogel strands conserves the spin and the energy, the collision integral vanishes for equilibrium distribution function of the true quasiparticle energy $n_0(\epsilon)$. It is therefore possible to linearize the collision integral using $\delta\tilde{n} = n - n_0(\epsilon)$

$$I[n] = \int d\mathbf{p}' w(\mathbf{p}, \mathbf{p}') (\delta\tilde{n}' - \delta\tilde{n}).$$

Furthermore, the solution of the kinetic equation can be sought for in the form

$$\delta\tilde{n} = \frac{\partial n_0}{\partial \epsilon} \chi(\hat{\mathbf{p}}), \quad \hat{\mathbf{p}} = \mathbf{p}/p,$$

where χ depends on the direction of \mathbf{p} only. The kinetic equation becomes

$$-\psi^m \frac{\partial \epsilon}{\partial p^m} = v_F \int d\sigma(\hat{\mathbf{p}}, \hat{\mathbf{p}}') (\chi' - \chi), \quad (4)$$

where $d\sigma$ is the differential scattering cross section per unit volume.

The flux \mathbf{j}_M also vanishes for $n_0(\epsilon)$ and can be linearized as follows

$$j_M^l = \int \frac{d\mathbf{p}}{(2\pi\hbar)^3} \frac{\partial \epsilon}{\partial p^l} \delta\tilde{n} = -\frac{p_F^2}{(2\pi\hbar)^3} \int d\hat{\mathbf{p}} \chi(\hat{\mathbf{p}}) \hat{p}^l. \quad (5)$$

We now have all tools ready for the diffusion tensor calculation. The differential cross section $d\sigma$ depends on the microscopic aerogel structure and the properties of quasiparticle scattering by aerogel strands. Let us represent the aerogel as an array of infinite cylindrical strands with diameter d oriented in z direction and randomly distributed in xy plane with the surface density N . The porosity of such structure is therefore

$$p = 1 - \frac{\pi N d^2}{4}.$$

For the scattering on the cylinder walls we consider two opposite limits: diffuse and specular reflection.

21 Diffuse Reflection

After diffuse reflection all information about the velocity direction of the incident particle is lost. The scattering cross section on a unit wall area is

$$d\sigma_{\mathbf{m}} = -\frac{d\hat{\mathbf{p}}'}{\pi} \begin{cases} 0, & (\mathbf{m}\hat{\mathbf{p}}) > 0; \\ 0, & (\mathbf{m}\hat{\mathbf{p}}') < 0; \\ (\mathbf{m}\hat{\mathbf{p}})(\mathbf{m}\hat{\mathbf{p}}'), & \text{otherwise,} \end{cases}$$

where the unit vector \mathbf{m} is the outer normal to the surface element. For a system of z -aligned cylinders, this vector is uniformly distributed in xy plane. The differential scattering cross section for this system is obtained by integration

$$\begin{aligned} d\sigma &= \frac{Nd}{2} \int d\mathbf{m} \delta(m_z) d\sigma_{\mathbf{m}} = \\ &= \frac{Nd}{4\pi} \sin\theta \sin\theta' |\sin\Delta - \Delta \cos\Delta| d\hat{\mathbf{p}}', \end{aligned} \quad (6)$$

where $\Delta = \phi - \phi' \in (-\pi, \pi)$, and the spherical angles (θ, ϕ) and (θ', ϕ') correspond to $\hat{\mathbf{p}}$ and $\hat{\mathbf{p}}'$ respectively.

Generally, the diffusion tensor D^{lm} has three principal values. Due to the axial symmetry of the system, it can be characterized by the mere two distinct components D^{\parallel} and D^{\perp} . It is therefore sufficient to calculate the diffusion in two directions: along and across the aerogel axis. In the former case the kinetic equation (4) is

$$-\psi \cos\theta = \int (\chi' - \chi) d\sigma. \quad (7)$$

If we substitute (6) in (7) and use the fact that the distribution function does not depend on the polar angle ϕ , we get

$$-\frac{\pi\psi \cos\theta}{2Nd} = \int (\chi' - \chi) \sin\theta \sin^2\theta' d\theta'.$$

The solution of this equation

$$\chi = \frac{\psi}{Nd} \frac{\cos\theta}{\sin\theta}$$

should be substituted in (5) to get the flux

$$\begin{aligned} j_M &= -\frac{p_F^2 \psi}{(2\pi\hbar)^3 Nd} \int d\hat{\mathbf{p}} \frac{\cos^2\theta}{\sin\theta} = \\ &= -\frac{p_F^2 \psi}{8\pi\hbar^3 Nd} = -D_D^{\parallel} \frac{\partial M}{\partial z}, \end{aligned}$$

where

$$D_D^{\parallel} = (1 + F_0^a) \frac{\pi v_F}{4Nd} = \frac{\pi^2 (1 + F_0^a) v_F}{16} \frac{d}{1 - p}. \quad (8)$$

Similar procedure can be used to investigate the lateral diffusion. If ψ^m has only x component, then the kinetic equation has the form

$$-\psi \sin\theta \cos\phi = \int (\chi' - \chi) d\sigma.$$

It has a solution

$$\chi = \frac{16\psi}{Nd(\pi^2 + 16)} \cos\phi,$$

which leads to the magnetization flux

$$\begin{aligned} j_M^l &= -\frac{p_F^2}{(2\pi\hbar)^3} \frac{16\psi}{Nd(\pi^2 + 16)} \int d\mathbf{p} \cos^2 \phi \sin \theta = \\ &= -D_D^\perp \frac{\partial M}{\partial x}, \end{aligned}$$

where

$$\begin{aligned} D_D^\perp &= (1 + F_0^a) \frac{2\pi v_F}{(\pi^2 + 16)Nd} = \\ &= \frac{\pi^2 (1 + F_0^a) v_F}{2(\pi^2 + 16)} \frac{d}{1 - p}. \end{aligned} \quad (9)$$

The diffusion anisotropy is described by the ratio

$$D_D^\parallel / D_D^\perp = (\pi^2 + 16)/8 \approx 3.23. \quad (10)$$

22 Specular Reflection

Elementary scattering cross section on a unit smooth surface is

$$d\sigma_{\mathbf{m}} = -d\mathbf{p}'(\hat{\mathbf{p}}\mathbf{m}) \begin{cases} 0, & (\mathbf{m}\hat{\mathbf{p}}) > 0; \\ \delta(\hat{\mathbf{p}}' - \hat{\mathbf{p}} + 2\mathbf{m}(\hat{\mathbf{p}}\mathbf{m})) & \text{otherwise.} \end{cases}$$

For the array of cylinders we again integrate over possible \mathbf{m} orientations

$$\begin{aligned} d\sigma &= \frac{Nd}{2} \int d\mathbf{m} \delta(m_z) d\sigma_{\mathbf{m}} = \\ &= \frac{Nd}{4} \delta(\theta - \theta') \left| \sin \frac{\phi - \phi'}{2} \right| d\mathbf{p}'. \end{aligned} \quad (11)$$

The delta function guarantees the conservation of the z component of momentum. This means that strictly parallel specular cylinders do not obstruct the spin flow along the system axis. Corresponding component of the diffusion tensor D_S^\parallel (infinite in our model) is limited either by strand irregularities or quasiparticle-quasiparticle collisions. Here we formally calculate only lateral (finite) component of the diffusion tensor.

We again write down the kinetic equation

$$-\psi \sin \theta \cos \phi = \int (\chi' - \chi) d\sigma.$$

It has a solution

$$\chi = \frac{3\psi}{4Nd} \cos \phi,$$

which results in the magnetization flux

$$j_M^l = -\frac{3\psi}{4Nd} \frac{p_F^2}{(2\pi\hbar)^3} \int d\phi d\theta \sin^2 \theta \cos^2 \phi = -D_S^\perp \frac{\partial M}{\partial x},$$

where

$$D_S^\perp = (1 + F_0^a) \frac{3\pi v_F}{32Nd} = \frac{3\pi^2 (1 + F_0^a) v_F}{128} \frac{d}{1 - p}. \quad (12)$$

3. DETAILS OF EXPERIMENTS

We have used two samples of nafen with overall densities 90 and 243 mg/cm³ (nafen-90 and nafen-243). Their structure was investigated in [10]. The samples consist of strands with diameter of ≈ 8 nm and ≈ 9 nm correspondingly. The density of bulk Al₂O₃ is 4 g/cm³, this gives for the porosities of the samples 97.8% (nafen-90) and 93.9% (nafen-243).

The experimental chamber used in the present work was similar to the chamber described in [3]. It is made of Stycast-1266 epoxy resin and has two separate cells. The cuboid samples with characteristic sizes of 4 mm are placed freely in the cells, so that $\sim 70\%$ of each cell is filled with nafen.

Experiments were carried out using spin-echo technique in magnetic field ≈ 280 Oe (corresponding NMR frequency is ≈ 900 kHz) at pressure of 2.9 bar. In order to avoid a paramagnetic signal from solid ^3He on the surface of strands, the samples were preplated by ~ 2.5 atomic layers of ^4He . The strands of the samples were oriented parallel to the external steady magnetic field \mathbf{H} . Two gradient coils were used to apply the field gradient in directions parallel and perpendicular to the strands. The necessary temperatures were obtained by nuclear demagnetization cryostat and were measured by a quartz tuning fork. The temperature was determined in assumption that the resonance linewidth of the fork in normal ^3He is inversely proportional to the temperature [11]. We calibrated the fork at high temperature where the diffusion coefficient in aerogel should be the same as in bulk ^3He (using [12] as a reference).

Spin echo decay curves were obtained by standard two-pulse method: we measured amplitude of the echo after $\pi/2 - \tau - \pi/2$ pulses, where τ is the delay between pulses. The measurements were carried out at temperatures from 1.4 mK up to 60 mK for two directions of magnetic field gradient (parallel and perpendicular to the direction of aerogel strands) and at several values of the gradients ($0.24 \div 1.25$ Oe/cm).

4. RESULTS

Expression for the spin echo amplitude

$$I = I_0 \exp(-2\tau/T_2 - A\tau^3) \quad (13)$$

can be found from Bloch-Torrey equations [13]. With an obvious generalization for an anisotropic media, the coefficient A here is given by

$$A = \frac{2}{3} \gamma^2 D^{lm} G^l G^m, \quad (14)$$

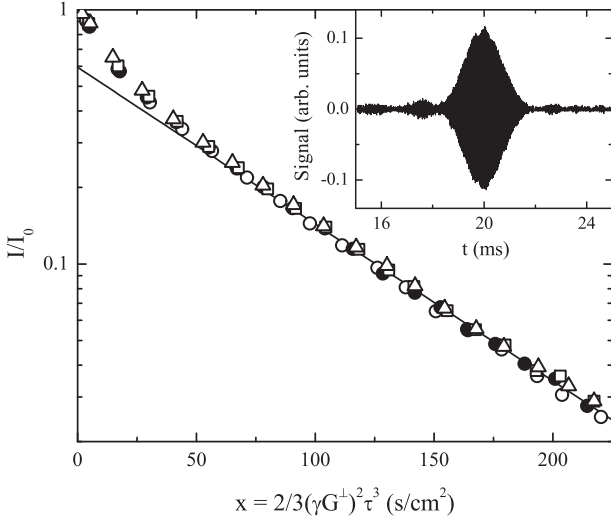


Fig. 1: Spin echo decay in ^3He in nafen-90 for different field gradients applied in direction perpendicular to aerogel strands. $G^\perp = 0.70$ Oe/cm (open circles), 0.53 Oe/cm (filled circles), 0.37 Oe/cm (open squares), 0.24 Oe/cm (open triangles). $H = 278$ Oe. $T \approx 2.0$ mK. Solid line is the best fit of the data at $x > 100$ by Eq.(13). Inset: Typical echo signal of ^3He in nafen-90. $T \approx 2.0$ mK, $G^\perp = 0.53$ Oe/cm, $\tau = 10$ ms.

where γ is the gyromagnetic ratio, G^l is the magnetic field gradient.

Typical echo signal of ^3He in nafen is shown in the inset in Fig.1. In order to determine the value of spin diffusion coefficient, spin echo amplitudes should be measured for different τ and then fitted by Eq.(13). In this procedure the term with T_2 can be neglected, because observed relationship between I/I_0 and $G^2\tau^3$ does not depend on field gradient at all used temperatures. An example data set is shown in Fig.1. Note that at $x \leq 80$ experimental points in Fig.1 deviate from the linear dependence. It is due to the presence of bulk ^3He outside the aerogel sample. At low temperatures the spin diffusion in bulk ^3He is greater than that in aerogel. However, for the same reason the relative contribution of bulk ^3He into the total echo signal rapidly decreases with the increase of τ , so we determined the value of spin diffusion coefficient $D(T)$ of ^3He in aerogel from the data at relatively large x where they follow the linear dependence ($x > 100$ for Fig.1).

The measured temperature dependencies $D(T)$ for two orientations of the gradient are shown in Fig.2 for nafen-90 and in Fig.3 for nafen-243. In order to obtain a value of spin diffusion coefficient in zero temperature limit ($D \equiv D(0)$) these dependencies were fitted by the equation

$$D^{-1}(T) = D_b^{-1}(T) + D^{-1}, \quad (15)$$

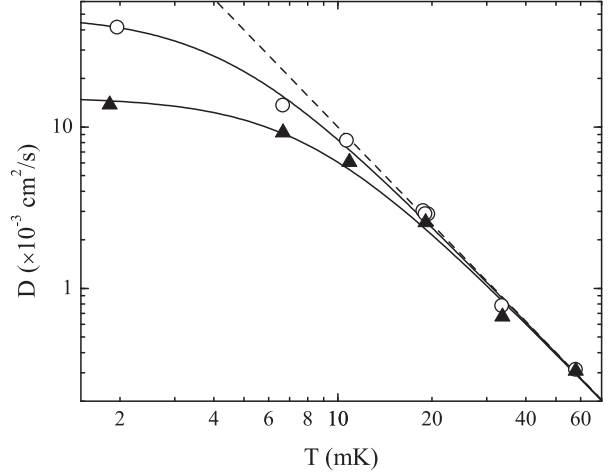


Fig. 2: Temperature dependence of the spin diffusion tensor: $D_{90}^{\parallel}(T)$ (open circles) and $D_{90}^{\perp}(T)$ (filled triangles) in nafen-90.

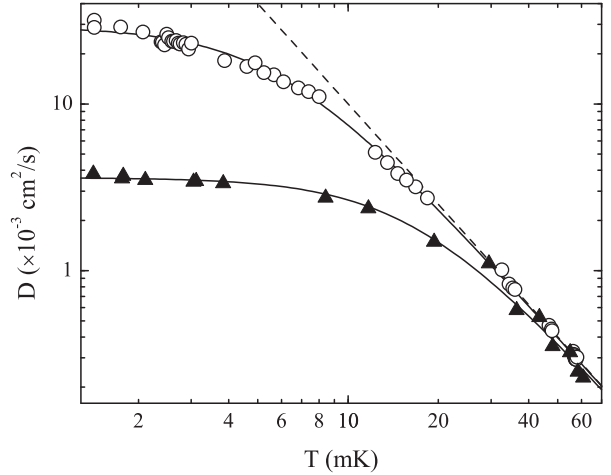


Fig. 3: Temperature dependence of the spin diffusion tensor: $D_{243}^{\parallel}(T)$ (open circles) and $D_{243}^{\perp}(T)$ (filled triangles) in nafen-243.

where $D_b \propto T^{-2}$ is the diffusion coefficient in bulk ^3He , which is determined only by collisions between quasiparticles. Solid lines in these graphs are fits by Eq.(15), dashed lines – diffusion coefficient in bulk ^3He (extrapolation to $P = 2.9$ bar using the data presented in [12]).

Obtained principal values of the spin diffusion tensor are:

- in nafen-90

$$D_{90}^{\parallel} \approx 0.049 \text{ cm}^2/\text{s},$$

$$D_{90}^{\perp} \approx 0.015 \text{ cm}^2/\text{s},$$

$$D_{90}^{\parallel}/D_{90}^{\perp} \approx 3.3.$$

- in nafen-243

$$\begin{aligned} D_{243}^{\parallel} &\approx 0.029 \text{ cm}^2/\text{s}, \\ D_{243}^{\perp} &\approx 0.0036 \text{ cm}^2/\text{s}, \\ D_{243}^{\parallel}/D_{243}^{\perp} &\approx 8.1. \end{aligned}$$

We estimate the accuracy of these values as $\pm 10\%$.

5. DISCUSSION

In isotropic system the spin diffusion coefficient is (see Eq.(1))

$$D = \frac{v_F \lambda}{3} v_F (1 + F_0^a). \quad (16)$$

As explained in Section 2 no mean free path can properly characterize the case of globally anisotropic aerogel. However, to account for the experimental data it is convenient to introduce zero-temperature effective mean free paths λ_{\parallel} and λ_{\perp} using Eq.(16) as the definition. If $v_F = 5397 \text{ cm/s}$ and $F_0 = -0.717$ [14] then for nafen-90 we get $\lambda_{\parallel} \approx 960 \text{ nm}$, $\lambda_{\perp} \approx 290 \text{ nm}$ and for nafen-243 $\lambda_{\parallel} \approx 570 \text{ nm}$, $\lambda_{\perp} \approx 70 \text{ nm}$.

In our experiments the strands of nafen were preplated with ^4He . In this case the reflection of quasiparticles on the surface is believed to be specular or at least partly specular [15, 16]. For specular reflection D_S^{\parallel} is limited by imperfect strands alignment and irregularities on their surface. Therefore we can not directly compare the measured ratio $k = D^{\parallel}/D^{\perp}$ with proposed theory for specular case. However, for nafen-243 we obtain $k \approx 8.1$ which is much greater than it is expected for diffuse one (see Eq.(10)). This means that the reflection in nafen-243 is predominantly specular.

The values of D_D^{\perp} and D_S^{\perp} can be calculated from Eqs.(9), (12) using values of ρ and d for our samples. These theoretical values should weakly depend on variations in orientations of the strands and can be compared with experiment. For the case of nafen-90 we obtain $D_S^{\perp} \approx 0.013 \text{ cm}^2/\text{s}$ and $D_D^{\perp} \approx 0.010 \text{ cm}^2/\text{s}$ while the experimental value $D_{90}^{\perp} \approx 0.015 \text{ cm}^2/\text{s}$. For nafen-243 $D_S^{\perp} \approx 0.0052 \text{ cm}^2/\text{s}$, $D_D^{\perp} \approx 0.0043 \text{ cm}^2/\text{s}$ and the experimental value $D_{243}^{\perp} \approx 0.0036 \text{ cm}^2/\text{s}$.

We can conclude that the experimental values qualitatively agree with the theoretical model. The quantitative difference may be due to experimental errors in determination of D , errors in nafen parameters, and variations of strands diameters (by $\pm 20\%$ as follows from [10]).

6. ACKNOWLEDGEMENTS

We are grateful to I.M. Grodnensky for providing the samples of nafen and to E.V. Surovtsev for useful discussions. This work was supported in parts by RFBR (grants 13-02-00674, 13-02-00912), Russian Science Support Foundation and the Basic Research Program of the Presidium of Russian Academy of Sciences.

1. D. Candela and D. Kalechofsky, J. of Low Temp. Phys. **113**, 351 (1998).
2. J.A. Sauls, Yu.M. Bunkov, E. Collin, H. Godfrin, P. Sharma, Phys. Rev. B **72**, 024507 (2005).
3. R.Sh. Askhadullin, V.V. Dmitriev, D.A. Krasnikhin, P.N. Martinov, A.A. Osipov, A.A. Senin, A.N. Yudin, Pis'ma v ZhETF **95**, 355 (2012) [JETP Lett. **95**, 326 (2012)].
4. R.Sh. Askhadullin, V.V. Dmitriev, P.N. Martynov, A.A. Osipov, A.A. Senin, A.N. Yudin, Pis'ma v ZhETF **100**, 747 (2014) [JETP Lett. **100**, 662 (2014)].
5. V.V. Dmitriev, A.A. Senin, A.A. Soldatov, E.V. Surovtsev, A.N. Yudin, ZhETF **146**, 1242 (2014) [JETP **119**, 1088 (2014)].
6. R.Sh. Askhadullin, P.N. Martynov, P.A. Yuditsev, A.A. Simakov, A.Yu. Chaban, E.A. Matchula, A.A. Osipov, J. Phys.: Conf. Ser. **98**, 072012 (2008).
7. <http://www.nafen.eu>
8. R.Sh. Askhadullin, V.V. Dmitriev, D.A. Krasnikhin, P.N. Martynov, L.A. Melnikovsky, A.A. Osipov, A.A. Senin, A.N. Yudin, J. Phys.: Conf. Ser. **400**, 012002 (2012).
9. D. Hone, Phys. Rev. **121**, 669 (1961).
10. V.E. Asadchikov, R.Sh. Askhadullin, V.V. Volkov, V.V. Dmitriev, N.K. Kitaeva, P.N. Martynov, A.A. Osipov, A.A. Senin, A.A. Soldatov, D.I. Chekrigina, A.N. Yudin, Pis'ma v ZhETF **101**, 613 (2015) [JETP Lett. **101**, to be published (2015)].
11. R. Blaauwgeers, M. Blazkova, M. Clovecko, V. Eltsov, R. de Graaf, J. Hosio, M. Krusius, D. Schmoranzner, W. Schoepe, L. Skrbek, P. Skyba, R. Solntsev, D. Zmeev, J. Low Temp. Phys. **146**, 537 (2007).
12. A.S. Sachrajda, D.F. Brewer, W.S. Truscott, J. Low Temp. Phys. **56**, 617 (1983).
13. A. Abragam, The principles of nuclear magnetism (Oxford: Oxford University Press), pp. 59-62 (1994).
14. <http://spindry.phys.northwestern.edu/he3.htm>
15. M.R. Freeman, R.S. Germain, E.V. Thuneberg, R.C. Richardson, Phys. Rev. Lett. **60**, 596 (1988).
16. M.R. Freeman, R.C. Richardson, Phys. Rev. B **41**, 11011 (1990).